DOI: 10.1002/adma.200801975

Nanoscale Ionic Materials**

By *Robert Rodriguez, Rafael Herrera, Lynden A. Archer,* and *Emmanuel P. Giannelis**

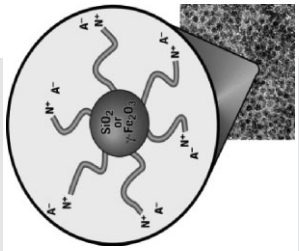

Polymer nanocomposites (nanoparticles dispersed in a polymer matrix) have been the subject of intense research for almost two decades in both academic and industrial settings. This interest has been fueled by the ability of nanocomposites to not only improve the performance of polymers, but also by their ability to introduce new properties. Yet, there are still challenges that polymer nanocomposites must overcome to reach their full potential. In this Research News article we discuss a new class of hybrids termed nanoparticle ionic materials (NIMS). NIMS are organic–inorganic hybrid materials comprising a nanoparticle core functionalized with a covalently tethered ionic corona. They are facilely engineered to display flow properties that span the range from glassy solids to free flowing liquids. These new systems have unique properties that can overcome some of the challenges facing nanocomosite materials.

1. Introduction

Polymer nanocomposites have attracted considerable attention in recent years. This interest is fueled by the promise of unprecedented performance, design flexibility, and lower unit and life-cycle costs. Current market forecasts estimate the use of nanocomposites to reach 45 million kilograms in 2011 ($500–800M), at an astonishing annual growth rate of 24%.[1] Despite this promise, and the consistent efforts by research groups world-wide, persistent challenges of poor miscibility, dispersion, and interfacial strength have prevented nanocomposites from realizing their full potential. New concepts such as the hybrids discussed here are required to break through the performance ceiling of current nanocomposites, and to create a basis for future advancements. This led to the development of hybrid materials based on surface-functionalized nanoparticles.[2] These hybrid systems, called nanoscale ionic materials (NIMS), are organic–inorganic hybrid particles comprising a charged oligomer corona attached to hard, inorganic nanoparticle cores (Fig. 1). An important consequence of this hybrid character is that the physical properties (rheological, optical, electrical, thermal) of NIMS can be tailored over an unusually broad range by manipulating geometric and chemical characteristics of the core and canopy (corona plus counterion species), as well as through thermodynamic state variables such as temperature and volume fraction.[2–8] Our recent work shows that by varying the molecular weight and grafting density of the canopy, a single NIMS system can be designed to display properties that continuously span the spectrum from glassy solids to simple, solvent-free, nanoparticle ionic fluids.[7,8] Because the effective fluidization medium (the canopy) in NIMS is tethered to the cores by strong primary ionic bonds, they make it possible to create new liquids with unusual combinations of properties. For example, NIMS comprising a high-refractive-index nanoparticle core densely grafted with short canopy chains provide new, even novel routes to liquids with zero-vapor pressure, low

[*] Prof. E. P. Giannelis, R. Rodriguez
Department of Materials Science and Engineering
Cornell University
Ithaca, NY 14853 (USA)
E-mail: epg2@cornell.edu
R. Herrera, Prof. L. Archer
School of Chemical and Biomolecular Engineering
Cornell University
Ithaca, NY 14853 (USA)

[**] We gratefully acknowledge support by the Cornell Center for Materials Research (CCMR), the Air Force Office of Scientific Research (AFOSR), and the Cornell University KAUST Center for Research and Education.

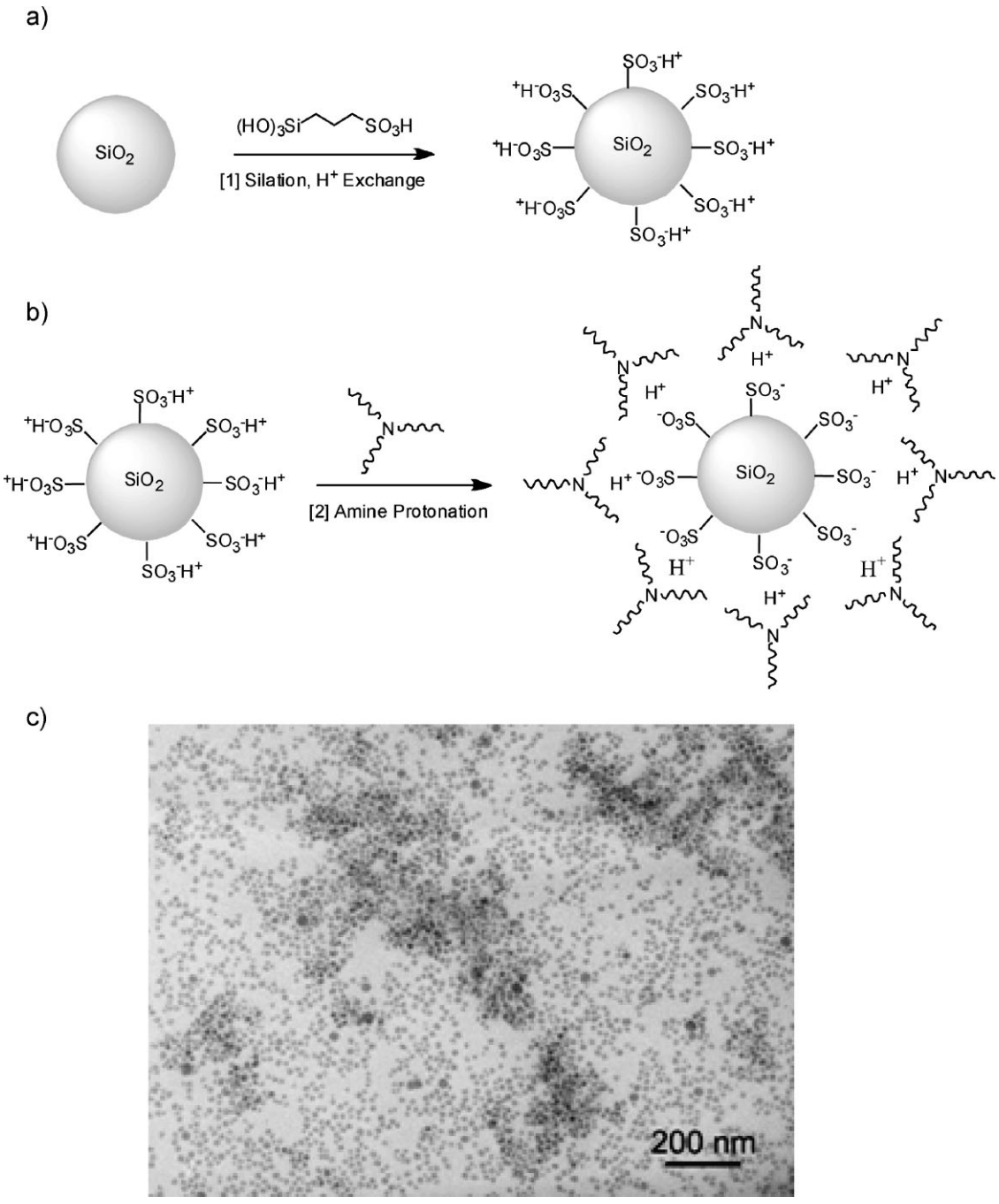

Figure 1. Schematic showing NIMS synthesis. a) First the nanoparticles are surface-functionalized by condensation with a sulfonate organosilane to form the corona. b) The acidic particles are neutralized with the tertiary amine (which serves as the canopy) in an acid–base reaction. c) TEM image showing monodispersed, unagglomerated nanoparticles (scale bar 200 nm).

viscosity, and high refractive index. They are therefore excellent candidate media for emerging applications in immersion photolithography.[9–11] Likewise, nanoparticle ionic fluids created from core particles with high electrical conductivity and mobile ionic species in the corona provide a new approach for creating stable, high-conductivity lubricating waxes and heat-transfer fluids,[12–14] and liquid electrolytes for high-temperature electrochemical cells.[15]

2. Nanoscale Ionic Materials

2.1. General NIMS Characteristics

NIMS are distinguished from conventional nanocomposites and colloidal suspensions in at least three ways. (i) The tethered corona and associated counterions are the suspending medium for the cores. This means that unlike a colloidal

ADVANCED MATERIALS

suspension where the suspending medium and the particles are physically distinct entities, each particle in a nanoparticle ionic fluid carries around its share of the suspending solvent. This arrangement is anticipated to produce profound differences in thermodynamic and scattering properties of the two types of fluids, and is expected to provide a stabilization mechanism for the NIMS cores that does not exist in a colloidal suspension. (ii) The hybrid nature of the fundamental units (building-blocks) facilitates straightforward design and synthesis of new, stable liquids with tunable properties. Specifically, by taking advantage of the large library of available inorganic chemistries for the cores, a single corona chemistry can be used to create an entire family of stable materials with a much wider spectrum of properties and applications than is possible with any colloidal suspension. (iii) The covalently attached corona and unscreened electrostatic charge stabilizes the NIMS core particles. This stabilization mechanism is different from that in typical colloidal suspensions where mobile charges in the suspensions migrate to the particle/fluid interface and screens electrostatic interactions between individual particles. An important consequence of (i) is that whereas removal of the suspending medium in a suspension occurs by breaking weak secondary bonds, solvent loss in an nanoparticle ionic fluid is resisted by strong primary bonds. This feature provides a potentially simple pathway to zero-vapor pressure liquids with unusual solvation characteristics (both the core and canopy can be harnessed for solute capture). It also means that temperature can be used to investigate correlations, ordering, and crystallization of the particle cores without concerns about solvent loss, which hamper such studies in colloidal suspensions.

2.2. First-Generation NIMS

First-generation NIMS are synthesized by grafting a charged, oligomeric corona onto the nanoparticle cores. For example, reaction of $(CH_3O)_3Si(CH_2)_3N^+(CH_3)(C_{10}H_{21})_2Cl^-$ with hydroxyl groups present on the surface of oxide nanoparticles leads to a permanent, covalent attachment of a corona onto the nanoparticles and renders the nanoparticles cationic.[7,8] Cl^- is initially present to balance the charge, in essence forming a nanoparticle salt. When chloride is the counter anion, the silica nanoparticles are in a solid form and show no phase transitions even after heating to 300 °C. In contrast, replacement of the chloride by sulfonate anions such as $(C_{13}H_{27}(OCH_2CH_2)_7O(CH_2)_3SO_3^-)$ yields a liquid at room temperature. If the counter anion is isostearate, $(CH_3(CH_3)CHCH_2(CH_2)_{12}CH_2COO^-)$, a gel-like material is obtained. Additional tunability can be achieved by exploiting the very large library of available inorganic cores. NIMS based on SiO_2, TiO_2, ZnO, γ-Fe_2O_3, C_{60}, carbon nanotubes (CNT), Au, Pt, and Pd nanoparticles have already been synthesized.[2–8,16]

Dielectric relaxation spectroscopy, Brillouin light scattering, shear rheometry, photoluminescent quenching, and X-ray scattering have been used to provide some insight into the structure and dynamics of two model silica nanoparticle fluids and their behavior.[6,17] The first system is based on isostearate as the counter anion while the other is based on sulfonate (see above). In both systems hard silica nanoparicle cores are surrounded by the same corona of flexible, positively charged aliphatic chains. The positive charges reside on the ammonium group, which is separated from the silica core by a short carbon atom spacer. Strong Coulombic and ion-pair interactions dictate that the anions are in close proximity to the ammonium groups, which are covalently attached to the nanoparticle surface by the short spacer. Thus, the size and nature of the anion are expected to significantly affect packing and, therefore, the fluidity of the system. In addition, owing to the hard–soft nature of the constituents as well as the presence of ionic and non-ionic domains, inhomogeneities at different length scales are anticipated, which should profoundly influence the physical properties of these materials.

Although the reasons for their fluidity are not yet completely understood, a working scenario is emerging.[6] According to this scenario the bulky and highly asymmetric ions in NIMS lead to frustrated molecular packing in the system and much weaker interactions than in the Cl^- analog. Using differential scanning calorimetry and dielectric spectroscopy we have reported that the glass transition temperature of the sulfonate and isostearate systems and, hence, the local dynamics are surprisingly similar, suggesting either weak anion association or free exchange of strongly bound anions on short time-scales in both systems. Despite the very similar local mobility, however, the two systems exhibit very different flow properties. Figure 6 in Reference [6] shows the master curve of the storage G' and loss G'' shear modulus for both systems as a function of reduced frequency, $a_T\omega$, at a fixed reference temperature of 273 K. Frequency reduction is performed using the time-temperature superposition principle. G' and G'' for both systems intersect at nearly identical frequencies ($\tau \approx 1$ ms at 273 K) suggesting that the same relaxation process is responsible for energy dissipation. At frequencies below the crossover point, however, the sulfonate based NIMS manifests a rapid transition to near terminal scaling behavior (i.e. $G'' \sim \omega > G'' \sim \omega^2$) characteristic of a dissipation-dominated or liquid state. In contrast, the isostearate system exhibits more complex behavior. While G'' is higher than G', indicating that the material more effectively dissipates than stores mechanical energy on times scale greater than 1 ms, the frequency dependence of modulus ($G'' > G' \sim \omega^{1/3}$) is intermediate between a disordered solid and a simple liquid. The more complex, gel–like flow behavior seen in the isostearate system relates to a liquid-like ordering observed by small-angle X-ray scattering. This enhanced structuring was also manifested as a second slow dynamic process in the dielectric loss spectrum.

2.3. Second-Generation NIMS

A complementary approach can be used for synthesizing NIMS based on oxide nanoparticles. This synthesis is scalable and can be used produce large quantities of material suitable for

applications. The first step involves surface functionalization of the particles by condensation of 3-(trihydroxysilyl)-1-propane sulfonic acid (SIT) with surface silanol groups as shown in Figure 1a. This charged organosilane renders the nanoparticles anionic, where a proton is present to provide charge neutrality to the system. In this form, the nanoparticles are white powders in the absence of solvents and show no visible phase transitions when heated to temperatures as high as 200 °C. As illustrated in Figure 1b, reaction of a strong acid in the form of the sulfonate functionalized silica nanoparticles with a tertiary amine $(C_{18}H_{37})N[(CH_2CH_2O)_mH]$ $[(CH_2CH_2O)_nH]$, which serves as a weak base, transforms the powders to neat amber-colored molten salts, the fluidity of which can be varied simply by controlling the volume fraction of cores. The transmission electron microscopy (TEM) image in Figure 1c shows non-aggregated particles consistent with the optical transparency of the samples.

Because the final synthetic step in NIMS involves the reaction of a strong acid with a weak base, the true equivalence point should occur at a pH below 7. Figure 2 shows the titration curve for the reaction between the surface-modified silica and tertiary amine. From the plot it is clear that the equivalence point for this particular set of functionalized nanoparticles occurs at pH ~ 4. Figure 2, therefore, serves as a phase diagram showing the transition from NIMS to a suspension of nanoparticles in excess amine, with the transition occurring at a core concentration corresponding to the equivalence point of the reaction. For this particular system, stoichiometric NIMS correspond to SiO_2 core concentration of 42 wt%. When an excess of the amine is present, it serves as a plasticizer increasing the fluidity of the system, and on the other end of the spectrum are materials with high nanoparticle core content, which display properties similar to waxes, gels, and glassy solids.

Figure 3a illustrates the effect of core particle concentration on the viscoelastic properties of NIMS at 28 °C. At a SiO_2 concentration of 19 wt%, Newtonian liquid behavior is observed as evidenced by the frequency-independent complex viscosity, $|\eta^*(\omega)|$ (lines). For modest increases in the SiO_2 concentration, complex viscoelastic behavior is observed through the frequency-dependent moduli and complex viscosity. In addition, steady-state shear rheometry reveals details about the interparticle interactions and Brownian motion of the cores. Figure 3b shows a plot of the viscosity as a function of shear stress for NIMS of varying core concentrations. Figure 3b illustrates that the post-yield flow properties of NIMS cover the full spectrum of complex fluid behavior; from simple Newtonian shear viscosity at low shear stresses to non-Newtonian shear-thinning at intermediate stresses and shear thickening at high stresses. Steady-state shear measurements indicate that even dense NIMS (35 wt%) show a solid-like yield at low shear stresses, $\tau_y = 0.25$ Pa, which is ca. 1/1000 of the elastic modulus G_{eq}, to produce a Newtonian liquid at low shear rates. It is also possible to estimate a characteristic structural relaxation time from the reciprocal of the shear rate at which the steady-state shear viscosity becomes shear-rate dependent. Measurements show that NIMS with a core

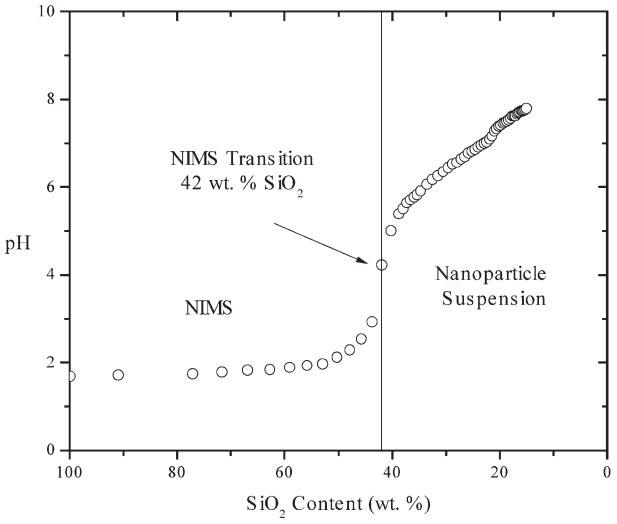

Figure 2. Titration curve for the reaction between surface modified silica and tertiary amine. The equivalence point for this system occurs at pH ~ 4 and corresponds to a SiO_2 concentration of 42 wt %.

concentration of 35 wt% have a characteristic relaxation time $\lambda_s = 4.1 \times 10^5$ s, which is much too large to result from a molecular process involving the organosilane and amine counter-ion species. This is most likely the timescale for Brownian motion of the surface-functionalized cores in the medium composed of the organosilane and amine species. Measurements of NIMS with a 19 wt% core concentration reveal characteristic relaxation times of about 5.0×10^{-2} s, much lower than those observed for NIMS with higher core contents. These observations nicely demonstrate the sensitivity of NIMS transport properties to the amount of cores present in each system.

Figure 3c is a plot of the relative viscosity ($\eta_r = \eta_0/\mu$, where η is the zero-shear viscosity of the suspension and $\mu = 0.21$ Pa s is the solvent viscosity) of NIMS as a function of core volume fraction. The relative viscosity of NIMS follows the same behavior as that observed in conventional colloidal suspensions, where the relative viscosity increases with increasing volume fraction (φ) until eventually diverging at a critical volume fraction associated with the glass transition.[13–14] Not only do these systems show similar behavior, but standard models such as the Krieger–Dougherty equation[18] and the Thomas equation[19] fit the data reasonably well, indicating that theories used for colloidal suspensions may satisfactorily describe the general behavior of these materials at concentrations below the NIMS transition. It is apparent from the figure that for $\varphi < 0.25$, both the Krieger formula and Thomas equation are in good accord with the experimental data, implying that at low concentrations these NIMS can be crudely modeled as suspensions, albeit with effective particle volume fractions larger than the volume fraction of the bare core. At higher φ, η_r diverges, and both models underpredict the relative viscosity. For a suspension of uncharged spheres, η_r diverges at $\varphi \approx \varphi_G = 0.58$, which is substantially higher than what is seen in NIMS. Independent dynamic rheology measurements per-

ADVANCED MATERIALS

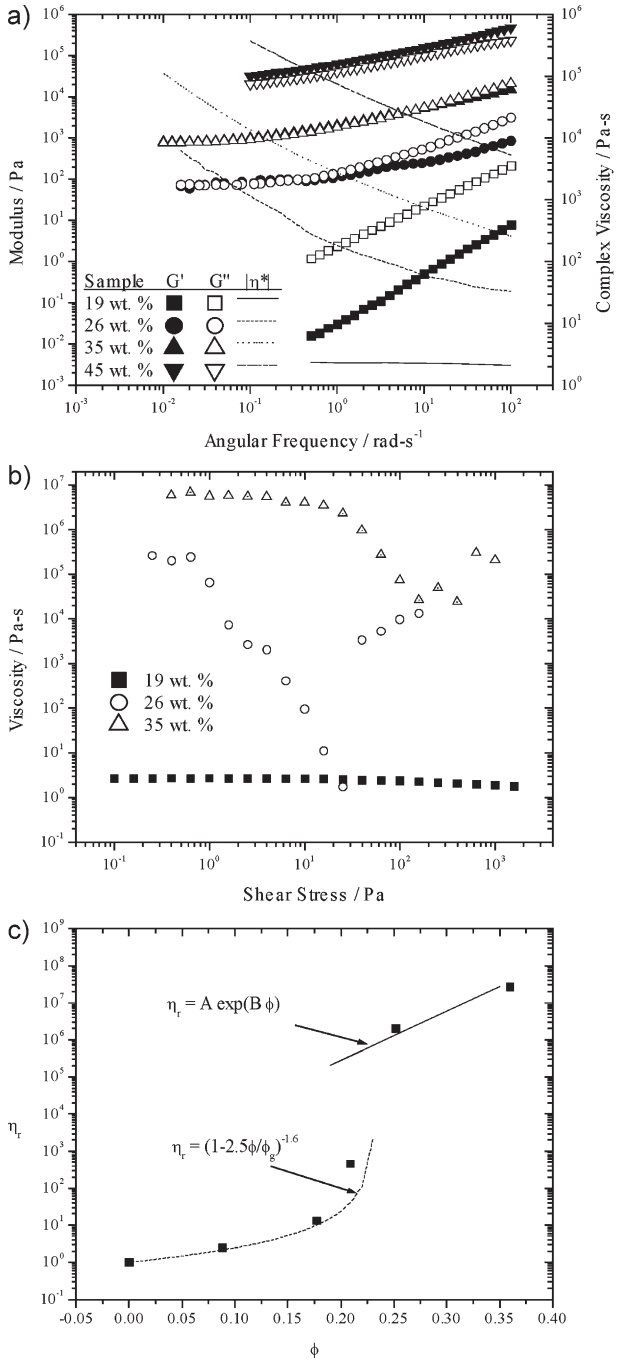

Figure 3. a) Viscoelastic properties of NIMS with variable nanoparticle core concentrations. Left axis: Storage modulus $G'(\omega)$ (closed symbols), and loss modulus $G''(\omega)$ (open symbols). Right axis: complex viscosity $|\eta^*(\omega)|$. *b*) Flow curves for NIMS at different core concentrations. c) Relative viscosity of NIMS as a function of effective core volume fraction.

formed at fixed oscillation frequency and variable shear strain γ reveal a frequency-dependent maximum in the loss modulus $G''(\omega)$ in NIMS with $\varphi \geq 0.2$, a feature firmly established as a characteristic of gel-like or glassy fluids.[20] This confirms that the divergence in η_r is the result of an earlier-than-expected transition to a glass or gel.

3. Conclusions

Our work shows that it is possible to synthesize nanoparticle ionic materials based on organic–inorganic hybrid particles with a wide range of physical properties. The hybrid nature of NIMS allows for a variation in the choice of core particle, corona, and canopy to create materials with properties specific to a wide range of applications. By varying the molecular weight and grafting density of the canopy, NIMS can be designed to display properties that continuously span the spectrum from glassy solids to simple, solvent-free, nanoparticle ionic fluids. The differences in the stabilization mechanisms between NIMS and conventional colloids and nanocomposites leads to zero-vapor-pressure liquids with potentially unusual solvation characteristics. Here we demonstrate a complementary approach for synthesizing NIMS. The new approach consists of an acid-base reaction between 3-(trihydroxysilyl)-1-propane sulfonic acid functionalized silica nanoparticles and an amine. Because of its simplicity the procedure can easily be scaled up to produce large quantities of materials. The equivalence point of the reaction between the acidic particles and the basic amine can be used to synthesize stroichiometric NIMS with a ratio of 1:1 of nanoparticle cores to counter ions. Additionally the equivalence point can be used to determine the transition from nanoparticle rich to NIMS containing excess amine. NIMS below the equivalence point behave similarly to suspensions of nanoparticles while materials above are more like gels. Rheological characterization indicates that the entire range of complex fluid behavior (i.e. from simple Newtonian liquids to complex viscoelastic materials) can be accessed in NIMS. Further studies are currently underway to correlate structure and dynamics of NIMS to their transport properties.

Experimental

Surface-Functionalized Ionic Nanoparticles: In one flask, Ludox HS 30 (Sigma Aldrich) colloidal silica (3 g) was diluted with deionized water (22 mL). At the same time 3-(trihydroxysilyl)-1-propane sulfonic acid (SIT, 40 wt %, Gelest) (4 g) was diluted with deionized water (20 mL). The silica suspension was slowly added to the SIT suspension while stirring vigorously. To this mixture a solution of sodium hydroxide (1 M) was added dropwise until the reaction pH was about 5. The entire solution was then heated to 70 °C and stirred vigorously for 24 h. After that, the suspension was placed into SnakeSkin dialysis tubing (10k MWCO, Pierce) and dialyzed using deionized water for 48 h. After dialysis, the functionalized silica solution was run through an ion exchange column (Dowex, HCR-W2 ion exchange resin) to remove Na^+ ions and fully protonate the sulfonate groups present. NIMS were prepared by dissolving a desired amount of Ethomeen 18/25 ($(C_{18}H_{37})N[(CH_2CH_2O)_mH][(CH_2CH_2O)_nH]$, Azko-Nobel) in deionized water to a concentration of 10 wt%. The Ethomeen 18/25 solution was then added dropwise to the silica solution while monitoring the pH. Once the silica and amine were reacted, the solvent was slowly removed by placing the solution in a vacuum oven and drying at 35 °C until all the water is removed. Equivalence point plots were used to determine the 1:1 ratio of nanoparticle cores/counter ion and synthesize stoichiometric NIMS as well as NIMS with varying nanoparticle core content below and above the equivalence point.

ADVANCED MATERIALS

Instrumentation: TGA measurements were obtained on a TA Instruments model Q500 under N_2 flow. Bright-field TEM images were obtained at 120 kV with a FEI Tecnai T12 Spirit Twin TEM/STEM. The TEM images were taken by dissolving the material in acetone, placing a few drops of the dispersion on a copper grid and evaporating the solvent. Rheological measurements were obtained on an ARES Rheometer and Paar Physica Modular Compact Rheometer 300 (MCR300). For both rheometers, a cone and plate measurement system was employed with a 25 mm diameter and 4.5° cone angle. All measurements were made at 28 °C. For the oscillatory shear tests, strain amplitudes less than 1% were used to ensure that the deformations are in the linear viscoelastice regime. Flow curves for all samples were obtained using a combination of steady shear tests on the ARES and creep experiments on the MCR300.

Published online: August 27, 2008

[1] K. I. Winey, R. A. Vaia, *MRS Bull.* **2007**, *32*, 314.
[2] A. B. Bourlinos, K. Raman, R. Herrera, Q. Zhang, L. A. Archer, E. P. Giannelis, *J. Am. Chem. Soc.* **2004**, *126*, 15358.
[3] A. B. Bourlinos, S. R. Chowdhury, R. Herrera, D. D. Jiang, Q. Zhang, L. A. Archer, E. P. Giannelis, *Adv. Funct. Mater.* **2005**, *15*, 1285.
[4] A. B. Bourlinos, S. R. Chowdhury, D. D. Jiang, Y. U. An, Q. Zhang, L. A. Archer, E. R. Giannelis, *Small* **2005**, *1*, 80.
[5] A. B. Bourlinos, V. Georgakilas, V. Tzitzios, N. Boukos, R. Herrera, E. R. Giannelis, *Small* **2006**, *2*, 1188.
[6] A. B. Bourlinos, E. P. Giannelis, Q. Zhang, L. A. Archer, G. Floudas, G. Fytas, *Eur. Phys. J. E* **2006**, *20*, 109.
[7] A. B. Bourlinos, R. Herrera, N. Chalkias, D. D. Jiang, Q. Zhang, L. A. Archer, E. P. Giannelis, *Adv. Mater.* **2005**, *17*, 234.
[8] A. B. Bourlinos, A. Stassinopoulos, D. Anglos, R. Herrera, S. H. Anastasiadis, D. Petridis, E. P. Giannelis, *Small* **2006**, *2*, 513.
[9] J. H. Burnett, *J. Photopolym. Sci. Technol.* **2005**, *18*, 655.
[10] M. Maenhoudt, G. Vandenberghe, M. Ercken, S. Cheng, P. Leunissen, K. Ronse, *J. Photopolym. Sci. Technol.* **2005**, *18*, 571.
[11] M. Switkes, M. Rothschild, *J. Vac. Sci. Technol. B* **2001**, *19*, 2353.
[12] S. P. Jang, S. U. S. Choi, *Appl. Phys. Lett.* **2004**, *84*, 4316.
[13] J. J. Vadasz, S. Govender, P. Vadasz, *Int. J. Heat Mass. Tran.* **2005**, *48*, 2673.
[14] H. Q. Xie, J. C. Wang, T. G. Xi, Y. Liu, F. Ai, Q. R. Wu, *J. Appl. Phys.* **2002**, *91*, 4568.
[15] B. Smarsly, H. Kaper, *Angew. Chem. Int. Ed.* **2005**, *44*, 3809.
[16] S. C. Warren, M. J. Banholzer, L. S. Slaughter, E. P. Giannelis, F. J. DiSalvo, U. B. Wiesner, *J. Am. Chem. Soc.* **2006**, *128*, 12074.
[17] B. H. Han, M. A. Winnik, A. B. Bourlinos, E. P. Giannelis, *Chem. Mater.* **2005**, *17*, 4001.
[18] I. M. Krieger, T. J. Dougherty, *T. Soc. Rheol.* **1959**, *3*, 137.
[19] D. G. Thomas, *J. Coll. Sci. Imp. U. Tok.* **1965**, *20*, 267.
[20] V. Tirtaatmadja, K. C. Tam, R. D. Jenkins, *Macromolecules* **1997**, *30*, 1426.